INSTITUTE OF PHYSICS PUBLISHING JOURNAL OF OPTICS B: QUANTUM AND SEMICLASSICAL OPTICS
J. Opt. B: Quantum Semiclass. Opt. **6** (2004) 28–33 PII: S1464-4266(04)60978-5

Measurements of diffusion resonances for the atom optics quantum kicked rotor

M E K Williams[1], M P Sadgrove[1], A J Daley[2], R N C Gray[1], S M Tan[1], A S Parkins[1], N Christensen[3] and R Leonhardt[1]

[1] Department of Physics, University of Auckland, Private Bag 92019, Auckland, New Zealand
[2] Institut für Theoretische Physik, Universität Innsbruck, A-6020 Innsbruck, Austria
[3] Physics and Astronomy, Carleton College, Northfield, MN 55057, USA

Received 17 March 2003, accepted for publication 29 September 2003
Published 13 October 2003
Online at stacks.iop.org/JOptB/6/28 (DOI: 10.1088/1464-4266/6/1/005)

Abstract
We present experimental observations of diffusion resonances for the quantum kicked rotor with weak decoherence. Cold caesium atoms are subject to a pulsed standing wave of near-resonant light, with spontaneous emission providing environmental coupling. The mean energy as a function of the pulse period is determined during the late-time diffusion period for a constant probability of spontaneous emission. Structure in the late-time energy is seen to increase with physical kicking strength. The observed structure is related to Shepelyansky's predictions for the initial quantum diffusion rates.

Keywords: quantum chaos, kicked atoms, laser-cooled atoms

1. Introduction

The atom optics realization of the kicked rotor has enabled the experimental study of the transition between quantum and classical behaviour for this fundamental non-linear system. For example, the effects of decoherence, the mechanism whereby quantum interference effects are destroyed via environmental coupling [1], have been studied in the quantum system. More classical-like behaviour is observed when decoherence is added, either by spontaneous emission events [2–4], amplitude noise [5, 6] or timing noise [7, 8]. However, recent theoretical studies have concentrated on what is perhaps a more direct approach to studying the quantum-to-classical transition—varying the action of the system and thereby the effective Planck constant, i.e. increasing the action to investigate the limit in which '$\hbar$' $\rightarrow$ 0 [9, 10]. Of particular interest is the behaviour found for intermediate values of '$\hbar$', for which regions of enhanced diffusion (diffusion 'resonances') are predicted to exist by simulations and analytical results.

These theoretical studies have concentrated on the case where the classical stochasticity parameter of the system stays the same and only the effective Planck constant is varied. However, in cold atom kicked rotor experiments, the most accessible parameter regime exists for the situation where the power in the kicking laser is held constant instead, while the pulsing period (which is proportional to the effective Planck constant) is changed. Numerically, it is found that this gives rise to different but analogous diffusion resonances from those found in the aforementioned simulations. Here, we present observations of diffusion resonances in this experimentally accessible regime, the structure of which can be traced to a scaling formula for the initial quantum diffusion rate derived by Shepelyansky [11]. The experimental results exhibit markedly different behaviour from that predicted by classical calculations. An increase in the complexity of the resonance structure is seen as the physical kicking strength is increased. Experimentally, the resonances are slightly diminished due to the non-uniform intensity profile of the kicking laser, but the expected structure is still clearly visible.

The resonances we observe are of a different nature from the quantum resonances previously studied in the atom optics kicked rotor[4], showing non-trivial dependence on the kicking strength as well as the scaled Planck constant. In particular, we note that the emphasis of our study is different from that of the related work by d'Arcy *et al* [12] which focused on such quantum resonance behaviour and not on the diffusion resonance behaviour at intermediate values of $\hbar$. Additionally, we note the difference between our experiments and those of

[4] The simplest quantum resonances (which are also those that have been previously studied experimentally) occur when the scaled Planck constant is an integer multiple of 2π.

Klappauf *et al* [13] in which anomalous diffusion behaviour was studied as a function of kicking strength for just a few values of the pulsing period. Our investigation is essentially the converse of this experiment: energies are measured as a function of the pulsing period for just a few values of a kicking strength parameter, and display a resonance structure which cannot be inferred from previous results.

The system and model that we study are presented in section 2, while the analysis of classical and quantum momentum diffusion in this system is discussed in section 3. Our experimental set-up is described in section 4, and the results (experimental, quantum and classical calculations) are presented in section 5. The conclusion is in section 6.

2. System and model

For our system we use a laser-cooled cloud of caesium atoms of initial temperature ≈20 μK interacting with a standing wave of off-resonant laser light. The laser is pulsed with period T and pulse profile $f(t)$. We note that the energy gained by the atoms during interaction with the off-resonant laser field is typically much greater than their thermal energy. Furthermore, numerical studies indicate that the effects we wish to observe are insensitive to the exact initial temperature over the range of approximately 1–100 μK [14] and thus the finite temperature of the cloud does not limit the investigation of diffusion resonances. If the detuning of the laser from the atomic transition is sufficiently large compared with the Rabi frequency of the transition (see section 4) the internal atomic dynamics can be eliminated and the motion of the caesium atoms is described by the single-particle Hamiltonian [15]

$$\hat{H} = \frac{\hat{p}^2}{2m} - \frac{\hbar\Omega_{\mathrm{eff}}}{8}\cos(2k_{\mathrm{L}}\hat{x})\sum_{n=0}^{N} f(t-nT), \qquad (1)$$

where $\hat{x}$ and $\hat{p}$ are operators representing the atomic position and momentum, respectively, and k_{L} is the wavenumber of the laser light. The effective potential strength (typically denoted by Ω_{eff} although it is not a physical Rabi frequency) is given by $\Omega_{\mathrm{eff}} = \Omega^2(s_{45}/\delta_{45} + s_{44}/\delta_{44} + s_{43}/\delta_{43})$. This expression accounts for dipole transitions between different combinations of hyperfine levels in the caesium atoms ($6S_{1/2}(F = 4) \rightarrow 6P_{3/2}(F' = 3, 4, 5)$), where δ_{ij} are the corresponding detunings between the laser and the atomic transition frequencies, and $\Omega/2$ is the resonant single-beam Rabi frequency. If we assume equal populations of atoms in all ground state Zeeman sublevels, then $s_{45} = \frac{11}{27}$, $s_{44} = \frac{7}{36}$, and $s_{43} = \frac{7}{108}$. It is useful to rewrite this Hamiltonian in appropriate dimensionless units as

$$\hat{\mathcal{H}} = \frac{\hat{\rho}^2}{2} - k\cos(\hat{\phi})\sum_{n=0}^{N} f(\tau - n), \qquad (2)$$

which is the usual expression for the Hamiltonian of the standard kicked rotor system. In these units—which will be referred to as 'scaled units'—the position operator is defined by $\hat{\phi} = 2k_{\mathrm{L}}\hat{x}$, the momentum operator is $\hat{\rho} = 2k_{\mathrm{L}}T\hat{p}/m$, time is rescaled as $\tau = t/T$, and our new Hamiltonian is related to equation (1) by $\hat{\mathcal{H}} = (4k_{\mathrm{L}}^2T^2/m)\hat{H}$. The classical stochasticity parameter is given by $\kappa = \Omega_{\mathrm{eff}}\omega_{\mathrm{r}}T\tau_{\mathrm{p}}$, where τ_{p} is the pulse length in unscaled time and $\omega_{\mathrm{r}} = \hbar k_{\mathrm{L}}^2/2m$. In our experiments, $f(\tau)$ is a good approximation to a square pulse, i.e. $f(\tau) = 1$ for $0 < \tau < \alpha$, where $\alpha = \tau_{\mathrm{p}}/T$. Note that $k = \kappa/\alpha$.

In scaled units we have $[\hat{\phi}, \hat{\rho}] = \mathrm{i}\bar{k}$, with $\bar{k} = 8\omega_{\mathrm{r}}T$, so that the quantum behaviour of our system is reflected by an effective Planck constant, $\bar{k}$, which increases as we increase the pulse period T. This reflects our ability to change the total action in the system, and hence how classically our system behaves (for larger $\bar{k}$ values the quantum nature of the system should be more apparent). Note that the effective Planck constant is proportional to the ratio of the total classical action of the system to $\hbar$.

The natural experimental unit for momentum is that of two photon recoils, $2\hbar k_{\mathrm{L}}$, and $p/(2\hbar k_{\mathrm{L}})$ will henceforth be referred to as the momentum in experimental units. We note the relationship $\rho/\bar{k} = p/(2\hbar k_{\mathrm{L}})$ and also define the quantity $\phi_{\mathrm{d}} = \kappa/\bar{k} = \Omega_{\mathrm{eff}}\tau_{\mathrm{p}}/8$ as a dimensionless measure of the physical kicking strength. Experimentally, it is easier to hold this quantity constant, rather than κ, as T is varied as a constant value of ϕ_{d} corresponds to constant pulse duration, standing wave detuning and power (whereas κ is proportional to T).

Our system is coupled to its environment via atomic spontaneous emission events, which occur when the caesium atoms absorb photons from the standing wave [2] and then spontaneously re-emit the photons in random directions. We characterize the level of this decoherence by the probability of spontaneous emission per atom per kick, η. Given the large detuning, i.e. $\Omega_{\mathrm{eff}}/\delta \ll 1$, this process may be modelled by the following master equation for the density operator $\hat{w}$ of the system [3]

$$\dot{\hat{w}} = -\frac{\mathrm{i}}{\bar{k}}[\hat{\mathcal{H}}, \hat{w}] - \frac{\eta}{\alpha}\sum_{n=0}^{N} f(\tau - n)[\cos^2(\hat{\phi}/2), \hat{w}]_+ + 2\frac{\eta}{\alpha}\sum_{n=0}^{N} f(\tau - n)\int_{-1}^{1} \mathrm{d}u\, N(u)\mathrm{e}^{\mathrm{i}u\hat{\phi}/2} \times \cos(\hat{\phi}/2)\hat{w}\cos(\hat{\phi}/2)\mathrm{e}^{-\mathrm{i}u\hat{\phi}/2}, \qquad (3)$$

where $N(u)$ is the distribution of recoil momenta projected onto the axis of the standing wave, and $[\cdot, \cdot]_+$ denotes an anti-commutator. Simulations of equation (3) are used for comparisons with the experiment.

3. Momentum diffusion

We measure the total kinetic energy of the cloud after N kicks, which depends on the initial energy of the cloud plus the increase in the kinetic energy resulting from the kicks. The amount of increase for kick number n is the momentum diffusion rate, given by $2D(n) = \langle\hat{\rho}_{n+1}^2\rangle - \langle\hat{\rho}_n^2\rangle$, where we denote $\hat{\rho}_0 = \hat{\rho}(t' = 0)$, $\hat{\rho}_1 = \hat{\rho}(t' = 1)$, etc. For a kicked rotor system with a sufficiently broad initial momentum distribution, we expect $D(0) = D(1) = \kappa^2/4$. The system then passes through an initial quantum diffusion period lasting typically for around five kicks [10], with a diffusion rate approximated by the result of Shepelyansky (under the conditions $\bar{k} \geqslant 1$ and $\kappa \gg \bar{k}$) [11],

$$D_{\mathrm{q}} = \frac{\kappa^2}{2}\left(\frac{1}{2} - J_2(K_{\mathrm{q}}) - J_1^2(K_{\mathrm{q}}) + J_2^2(K_{\mathrm{q}}) + J_3^2(K_{\mathrm{q}})\right), \qquad (4)$$

where $K_q = 2\kappa \sin(\bar{k}/2)/\bar{k}$. Note that the classical diffusion rate is also given by equation (4), but with $K_q \to \kappa$ (i.e., $\bar{k} \to 0$).

Without decoherence, the system generally settles into a localized state [16], but the loss of phase coherence produced by the addition of spontaneous emission causes the system to settle instead into a final steady-state diffusion regime, with a late-time diffusion rate which may be approximated by the formula [2, 10, 16]

$$D_\infty = \sum_{n=0}^{\infty} \eta(1-\eta)^n D_0(n), \tag{5}$$

where $D_0(n)$ is the diffusion rate at the nth kick for a kicked rotor *without* decoherence. Essentially, this formula assumes that dynamical correlations over particular time intervals which give rise to the late-time diffusion rates are suppressed by a factor equal to the probability that a spontaneous emission occurs within that time interval. The correlations taken over a set number of kicks give rise to the diffusion rates seen in the kicked rotor without decoherence after that number of kicks, which leads to the late-time diffusion rate being an appropriate weighted average over the diffusion rates as the kicked rotor 'settles down' [10]. Thus, the diffusion rates in the first few kicks are essentially 'locked in' by the spontaneous emission events, and we observe similar structure in the late-time diffusion rates as we vary T to that observed in the initial quantum diffusion rates. This phenomenon has been confirmed by simulations of late-time diffusion rates [10], and although it is not directly tested by the experiment described here (since final energies are measured rather than diffusion rates) our measurements do show the behaviour that is expected if similar behaviour to that seen in the early-time diffusion regime is being reproduced in the late-time regime.

The structure predicted in the initial quantum diffusion rates as we vary T for constant ϕ_d, with diffusion rates measured in experimental units, is particularly interesting. We can express Shepelyansky's formula in this regime as

$$D'_q = \frac{(\phi_d)^2}{2}\left(\frac{1}{2} - J_2(K'_q) - J_1^2(K'_q) + J_2^2(K'_q) + J_3^2(K'_q)\right), \tag{6}$$

with $K'_q = 2\phi_d \sin(4\omega_r T)$. We then see that any structure in the diffusion rates is periodic in T with period $2\pi/8\omega_r$. (In fact, from equation (5) this is also true for the late-time diffusion rates.) We also see that the form of the structure depends solely on the value of ϕ_d. Figure 1 shows the initial quantum diffusion rate as a function of pulse period for varying values of ϕ_d. We see the regular feature of a peak near the quantum resonance at $\bar{k} = 2\pi/8\omega_r$ ($T = 60.4$ μs), and we see increasing numbers of enhanced diffusion peaks or resonances as we increase the value of ϕ_d.

The classical diffusion rate can be similarly found in this regime to be

$$D'_{cl} = \frac{(\phi_d)^2}{2}\left(\frac{1}{2} - J_2(\kappa) - J_1^2(\kappa) + J_2^2(\kappa) + J_3^2(\kappa)\right), \tag{7}$$

with $\kappa = 8\omega_r T \phi_d$. The second set of curves in figure 1 shows the classical rate for various ϕ_d. These rates oscillate around the quasilinear value which in these units is $(\phi_d)^2/4$, with the oscillations increasing in frequency with ϕ_d. For any given ϕ_d however, the structure in the classical diffusion rate is markedly different from that seen in the initial quantum rate.

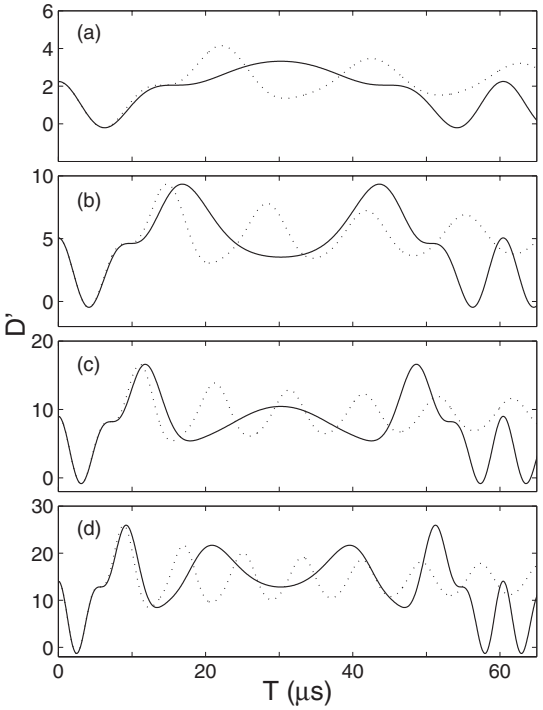

Figure 1. Theoretical initial momentum diffusion rates in the quantum case (solid curve), D'_q as given by equation (6), and the classical case (dotted curve), D'_{cl} in equation (7), in experimental units of as a function of T for (a) $\phi_d = 3$, (b) $\phi_d = 4.5$, (c) $\phi_d = 6$ and (d) $\phi_d = 7.5$. The quantum resonance is seen in the quantum diffusion rate at $T = 60.4$ μs.

In the experiment, late-time energies were measured and not initial diffusion rates. However, the diffusion resonances discussed above are still observable. The existence of the same structures in the late-time diffusion rates (in the presence of decoherence) as those predicted in the initial quantum rates has been verified using the simulations described later in this paper. From the definition of the diffusion rate, the energy after N kicks can be found by summing the diffusion rate at each kick, that is

$$E'(N) = \frac{\langle (p/2\hbar k_L)^2 \rangle}{2} = \sum_{n=0}^{N-1} D'(n, T). \tag{8}$$

Therefore, with the initial and final diffusion rates both displaying these structures, it follows that the energy at the Nth kick should also display them.

4. Experiment

The experimental set-up used was much the same as that used previously in our quantum chaos investigations [2, 17], with a few modifications. A standard six-beam magneto-optical trap (MOT) was used to trap and cool approximately 10^5 caesium atoms. The trapping laser frequency was set about 10 MHz to the red of the $6S_{1/2}(F = 4) \to 6P_{3/2}(F' = 5)$ transition. A second (repump) laser was locked to the $6S_{1/2}(F = 3) \to$

$6P_{3/2}(F' = 4)$ transition to return those atoms lost to the $F = 3$ ground state to the trapping cycle. After a 20 ms cooling phase prior to kicking, the cloud had a temperature of approximately 20 μK and a width of $\sigma_{\text{cloud}} \sim 270$ μm in its position distribution. Kicking of the cloud occurred for up to 2 ms during the 10 ms free expansion phase, at the completion of which the cloud was 'frozen' in space by the molasses beams and imaged. The repumping beam was left on during the kicking to prevent loss of atoms to the $F = 3$ ground state. The resultant heating effect was negligible for our experiments.

A third laser was used to create a pulsed optical standing wave across the cloud. A 150 mW laser diode was injection locked with a frequency-stabilized external cavity laser, giving a beam of up to 22 mW CW power at the MOT. For fast switching the beam passed through a 80 MHz acousto-optic modulator (AOM) in front of a single mode polarization preserving optical fibre. Temporal modulation was provided via the RF supply to the AOM, generating pulse shapes very close to rectangular. The linearly polarized beam was then collimated giving a beam radius at the cloud of $2\sigma_{\text{beam}} = 1$ mm. Finally, to create a standing wave the beam was retroreflected by a mirror outside the vacuum cell. The atoms experienced a range of optical potential depths as the cloud's width was comparable in size to that of the laser beam. If $\phi_{\text{d,max}}$ is the kicking strength along the beam axis then the mean value was found to be $\phi_{\text{d,mean}} \approx 0.77\phi_{\text{d,max}}$ with a standard deviation of 18%. In the following, ϕ_{d} will always refer to $\phi_{\text{d,mean}}$. The detuning of the kicking beam to the blue of the $F = 4 \rightarrow F' = 5$ transition was monitored as a beat frequency of the superposition of the trapping and kicking beams. Both the beam detuning and intensity were chosen to give a desired ϕ_{d} while maintaining a constant spontaneous emission rate. The range of ϕ_{d} examined in this way was from $\phi_{\text{d}} = 3.3$ to 6.6. Taking reflection losses at the cell windows into account, over this ϕ_{d} range the Rabi frequency varied from $\Omega/2\pi = 34$–76 MHz with corresponding detunings of $\delta_{45}/2\pi = 315$–740 MHz, thus $\delta \gg \Gamma, \Omega$ was satisfied for all ϕ_{d} values considered.

For a chosen ϕ_{d} the pulse length was held constant ($\tau_{\text{p}} = 520$ ns), while the pulse period was varied from 2.5 μs to just above the quantum resonance at $T \approx 60$ μs. Thirty kicks were delivered to the cloud for each pulse period. The images of the expanded cloud were averaged over the dimension perpendicular to the kicking beam to yield the momentum distributions for the kicked cloud and the mean energy $E = \langle p^2 \rangle/2$ was calculated for each distribution. High momenta have a large effect on these energy values and as this was where the signal dropped for the higher energy kicked clouds, much care was taken to reduce the effects of noise. For an experimental run involving a single ϕ_{d} value, the subtracted background was an average from just before and after the run. Any slight fluctuations in background level were accounted for by defining the zero level for each momentum distribution via an image taken just before commencement of the kicking sequence, omitting the small cloud. The signal-to-noise ratio was on average about 100:1 and for each value of T the momentum distribution was measured five times. To minimize the effects of long-term fluctuations in the kicking beam, one fibre end was angle cleaved and the beam power was checked and readjusted several times throughout a run. These measures reduced the fluctuations in ϕ_{d} from this source to ∼1%.

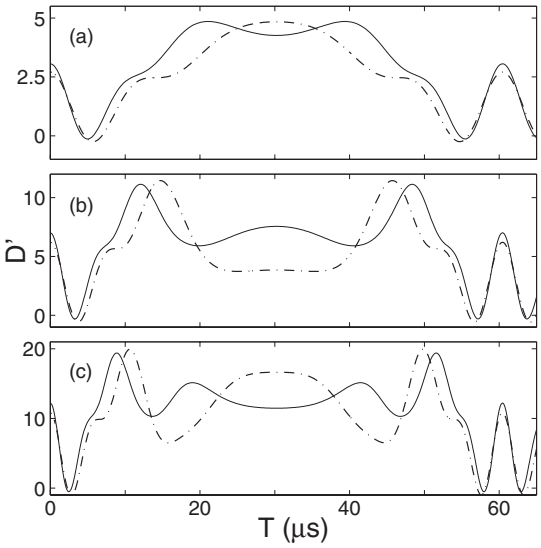

Figure 2. Initial momentum diffusion rates, D', with constant ϕ_{d} (dash–dotted curve) and the experimental spread in ϕ_{d} (solid curve) in experimental units as a function of T for (a) $\phi_{\text{d}} = 3.3$, (b) $\phi_{\text{d}} = 5.0$ and (c) $\phi_{\text{d}} = 6.6$.

We now examine the causes of the experimental spread in kicking strength and the effect of this spread on early-time diffusion rates. Firstly, there is a spread in physical kicking strengths due to the finite width of the kicking beam, which results in atoms at different radial positions across the beam interacting with laser fields of different intensity. The effect of the spread in kicking strengths on the initial Shepelyansky diffusion rates is easily examined and also applies to the late-time energies. If $\rho(r)$ is the two-dimensional cloud density as a function of radius r, and $\phi_{\text{d}}(r)$ the distribution of kicking strengths, then we define the diffusion rate for a given $\phi_{\text{d,max}}$ as [7]

$$\bar{D}(\phi_{\text{d,max}}, T) = \int_0^\infty D(\phi_{\text{d}}(r), T)\rho(r)2\pi r \, \text{d}r, \qquad (9)$$

where $D(\phi_{\text{d}}(r), T)$ is given by equation (6). Calculating $\bar{D}(\phi_{\text{d,max}}, T)$ for a broad kicking beam with $\sigma_{\text{cloud}} \ll \sigma_{\text{beam}}$, corresponding to constant $\phi_{\text{d}}(r)$, reproduces the pronounced structure as seen in figure 1 and in the simulations. But calculating the diffusion rate with the 2:1 beam-to-cloud ratio as used experimentally, so that $\phi_{\text{d,max}} = \phi_{\text{d}}/0.77$, gives a less accentuated diffusion resonance structure. Figure 2 displays these results for a few values of ϕ_{d}. Thus, a spread in ϕ_{d} values creates an averaging effect which somewhat diminishes the height of the diffusion resonance structure and shifts the positions of the resonant peaks relative to the case for a single ϕ_{d} value.

Secondly, a spread in ϕ_{d} values is also caused by atoms in different magnetic substates of the $F = 4$ level coupling to the higher-energy states with different transition strengths, resulting in atoms in different substates experiencing different kicking strengths. The combination of this effect with that caused by the finite beam width can create a spread of ϕ_{d} values which is as large as 20% of the mean ϕ_{d} value. In order to

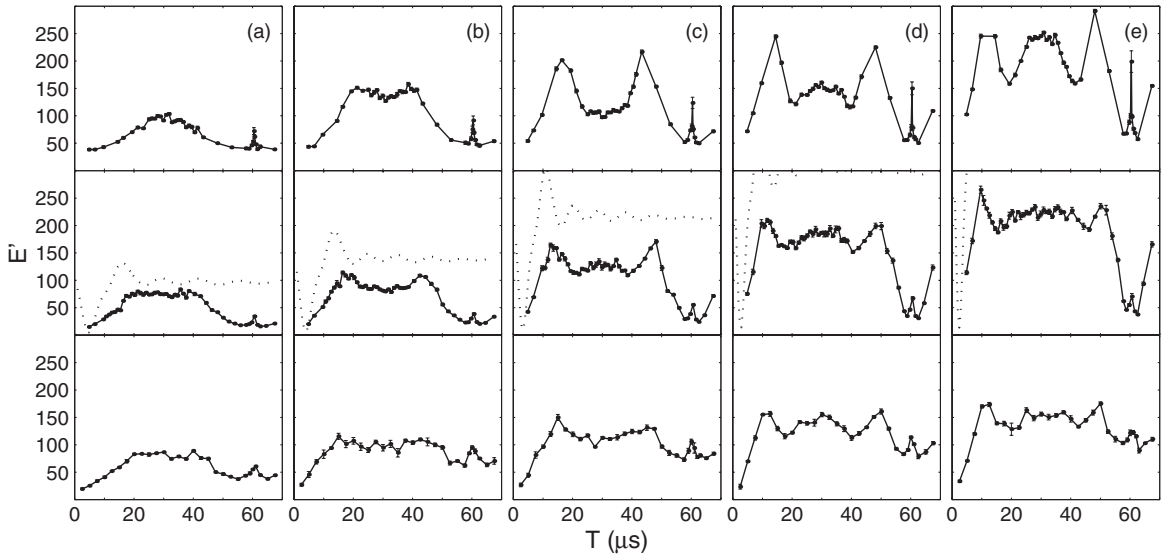

Figure 3. Quantum simulations with fixed ϕ_d (top) and the corresponding experimental results (bottom) giving the energy, E', after 30 kicks as a function of pulse period with $\tau_p = 520$ ns, $\eta = 0.0125$ for (a) $\phi_d = 3.3$, (b) $\phi_d = 4.0$, (c) $\phi_d = 5.0$, (d) $\phi_d = 5.9$ and (e) $\phi_d = 6.6$. Additional quantum simulations (middle, solid curve) take into account the spread in physical kicking strength ϕ_d, as do the analytical classical results (middle, dotted curve). The energies are in experimental units and error bars for the experimental and simulation results are shown but are very small.

account for this, we performed additional simulations in which the ϕ_d value for each trajectory was chosen from a distribution based on the 2:1 beam-to-cloud width ratio for our system (assuming that each has a radial Gaussian profile). Similarly, a random initial magnetic substate was selected for each trajectory (assuming equal populations in all substates) and ϕ_d was adjusted according to that substate's relative transition strength.

5. Experimental results

We have compared our experimental results with numerical simulations of equation (3). The simulations are performed using the method of quantum trajectories, as in [10]. The simulations reflect a system with an initial Gaussian distribution in momenta of width $\sigma_p/\bar{k} = \sigma_p/2\hbar k_l = 4$ (this corresponds to a cloud of temperature $\approx$20 μK). They also take into account the effects of finite pulse widths, spontaneous emission noise, and small amplitude fluctuations in the kicking strength.

To take into account the unavoidable spread of ϕ_d values in our experiments, simulations were also performed in which the kicking strength for each trajectory was sampled from the theoretical distribution of ϕ_d experienced by a spherical cloud of atoms (see section 4), and the energy for each value of T was taken to be the incoherent average of the energies over all such realizations. The results of these simulations are seen in the second row of figure 3. Comparison of the first two rows shows that while the non-uniformity of the kicking beam intensity makes the diffusion resonances somewhat less distinct, the structure of interest is still clearly visible and thus amenable to experimental investigation.

Comparison of experimental results with those from the simulations (bottom and middle rows of figure 3 respectively) shows good agreement between the two. The quantum resonance at $T \approx 60$ μs is seen to be present for all ϕ_d values. Additionally, while a single broad peak similar to that seen by d'Arcy *et al* [12] is found for $\phi_d = 3.3$, for larger ϕ_d values a more complicated structure is observed. This peak splits into two peaks which then diverge from each other, whereupon a third peak rises between them. The structure mirrors that in the initial quantum diffusion rate as given by Shepelyansky's result in equation (6) and shown in figure 1.

There is still some discrepancy in energy values between the experimental results and the additional simulations. For $\phi_d = 5.9$ and 6.6 the measured energies are overall much lower than expected, while for all ϕ_d they are much larger than in the simulations around the quantum resonance region of $T = 58$–68 μs. The first problem is accounted for by realizing that in recording the momentum distributions, at some point signals at higher momenta fall below the noise level of the CCD. Hence, the measured total energy of the cloud is systematically lower than the true energy after kicking. For larger ϕ_d, for which energies are higher in general, this problem is particularly pronounced as more atoms lie in the wings of the distribution. The discrepancy around the quantum resonance (seen at 60.4 μs), where the energies do not fall as low as expected to either side, currently remains unexplained, but could be a systematic effect related to the larger pulse period values in this region. Continuing investigations will hopefully resolve this issue.

Overall, agreement between the experimental results and the additional simulations is very good. Clear diffusion resonance structure is evident and the amount of detail increases with ϕ_d as expected. For comparison, the energies for the classical system after 30 kicks were also computed by assuming that the diffusion rate for the first two kicks is $\phi_d/4$, and for subsequent kicks is given by equation (7). They were averaged over the same spread in ϕ_d values that was used in the additional quantum simulations and are shown in the middle row of figure 3. Note that the energies are larger than the

quantum simulations, as is expected, and for $\phi_d = 5.9$ and 6.6 go off the scale, oscillating around $E' = 300$ and 560 respectively.

The classical energies clearly exhibit very different behaviour from those measured in the quantum system. The difference becomes more marked at higher values of T (i.e. when the system behaves more quantum mechanically), where the oscillations in the classical energy decrease in amplitude, whilst pronounced diffusion resonances and quantum resonances are seen in the quantum system. This can be contrasted with the results of Klappauf *et al* [13] where, in both the classical and quantum systems, the energy oscillates about the quasilinear value and only a relative shift in the peak positions distinguishes the two regimes. The striking difference between the quantum behaviour and the expected classical behaviour in these experiments makes them a thorough testing ground for the effects of decoherence on the quantum kicked rotor. Indeed, preliminary investigations into the effects of amplitude and period noise on these diffusion resonances [18] suggest that quantum and diffusion resonances are affected in different ways by the same type of noise.

6. Conclusion

We have presented experimental and simulation results showing non-trivial behaviour in the late-time energy (and thus diffusion rate) as the pulse period is varied for the quantum kicked rotor. Very good qualitative agreement between the results and simulations can be seen, and the relationship of the observed structure to Shepelyansky's formula for the initial quantum diffusion rates is evident. Furthermore, we note that the structure observable in the late-time energies agrees with numerical findings that in a system subject to environmental coupling a dependence of the late-time diffusion rate on the initial quantum diffusion rate exists.

Investigations are currently under way to discover the source of the remaining discrepancies between the simulations and experimental results. We have also begun studies of similar diffusion resonances found in the quantum kicked rotor with the addition of amplitude noise on the kick strength and noise on the period between kicks.

Acknowledgment

This work was supported by the Royal Society of New Zealand Marsden Fund, grant UOA016.

References

[1] Zurek W H 1991 *Phys. Today* **44** (October) 36
[2] Ammann H, Gray R, Shvarchuck I and Christensen N 1998 *Phys. Rev. Lett.* **80** 4111
[3] Doherty A C, Vant K M D, Ball G H, Christensen N and Leonhardt R 2000 *J. Opt. B: Quantum Semiclass. Opt.* **2** 605
[4] Klappauf B G, Oskay W H, Steck D A and Raizen M G 1998 *Phys. Rev. Lett.* **81** 1203
[5] Milner V, Steck D A, Oskay W H and Raizen M G 2000 *Phys. Rev.* E **61** 7223
[6] Steck D A, Milner V, Oskay W H and Raizen M G 2000 *Phys. Rev.* E **62** 3461
[7] Sadgrove M P 2002 *Master's Thesis* University of Auckland
[8] Oskay W H, Steck D A and Raizen M G 2003 *Chaos, Solitons Fractals* **16** 409
[9] Bhattacharya T, Habib S, Jacobs K and Shizume K 2002 *Phys. Rev.* A **65** 032115
[10] Daley A J, Parkins A S, Leonhardt R and Tan S M 2001 *Phys. Rev.* E **65** 035201
[11] Shepelyansky D L 1987 *Physica* D **28** 103
[12] d'Arcy M B, Godun R M, Oberthaler M K, Summy G S, Burnett K and Gardiner S A 2001 *Phys. Rev.* E **64** 056233
[13] Klappauf B G, Oskay W H, Steck D A and Raizen M G 1998 *Phys. Rev. Lett.* **81** 4044
[14] Daley A J 2002 *Master's Thesis* University of Auckland
[15] Raizen M G 1999 *Adv. At. Mol. Opt. Phys.* **41** 43
[16] Cohen D 1991 *Phys. Rev.* A **44** 2292
[17] Ammann H, Gray R, Shvarchuck I and Christensen N 1998 *J. Phys. B: At. Mol. Opt. Phys.* **31** 2449
[18] Sadgrove M, Hilliard A, Tan S and Leonhardt R, unpublished